

Variational ansatz using the LCT basis

Kyriakos Grammatikos

1 Project Lore

In LCT so far we have used a particular truncation scheme to reduce the infinite number of primaries that constitute the basis of the free boson/fermion in 1+1-D: operators are organized in blocks determined by two quantum numbers, the particle number n and the conformal dimension Δ and in each sector (n, Δ) , there is a certain number of operators $N(n, \Delta)$. Different sectors are orthogonal to each other. The number of operators in the basis can be made finite by imposing an upper limit to the scaling dimension of operators included in the basis $\Delta \leq \Delta_{\text{max}}$. This procedure effectively truncates the particle sector, due to the structure of the conformal basis chosen; in particular, the number of particles included in the basis is also limited by the truncation level: $n \leq \Delta_{\text{max}}$. What's more, this truncation scheme favors low energy particle sectors in general, and the particle sectors containing the largest number of operators are located near $\sim \sqrt{\Delta_{\text{max}}}$ for large truncation levels.

However, it has been shown in the past that to analytically reproduce non-perturbative phenomena like phase transitions, at least in theories where particle number is a good quantum number for the non-interacting theory, one needs to include information from arbitrarily high particle number sectors [3][1][2]. In previous work, we have seen that LCT is able to display signs of a phase transition, despite the assumption of a trivial vacuum; information about the failure of this ansatz is included in the excited modes above the vacuum.

In this work, our main goal is to study a new flavor of LCT, where states of arbitrarily high particle number are included in the basis from the get go. This can be achieved both numerically and analytically, by introducing special states that look somewhat like harmonic oscillator coherent states; each coherent state is a superposition of an infinite number of operators of quantum number $J = \Delta - n$.

The hope is that the variational techniques developed here will allow for an alternative, semianalytic way to determine the phase boundary, reduce computational effort compared to previous work and provide deeper insights into the results obtained there. Also, we hope that this will pave the way for understanding nonperturbative breaking in LCT more deeply, especially in models where there is no window of perturbative access to the breaking pattern, as is true in, for example, the Schwinger model in 1+1-D.

2 Methods

The idea is to define quantum states controlled by a single complex parameter

$$|z\rangle = \frac{1}{N(z)} \sum_{n=0}^{\infty} A_n z^n |\mathcal{O}_n, p\rangle \quad (2.1)$$

where the CFT operator states are constructed by Fourier transforming a chiral bosonic operator acting on the vacuum

$$|\mathcal{O}_n, p\rangle = \int_{-\infty}^{\infty} dx e^{-ipx} \mathcal{O}_n(x) |0\rangle \quad (2.2)$$

The states chosen are normalized as follows

$$\langle \mathcal{O}_m, p' | \mathcal{O}_n, p \rangle = 2\pi(2p) \delta(p - p') \delta_{mn} \quad (2.3)$$

Ideally, we want to pick the functions A_n and operators from the conformal boson basis such that their matrix elements with the Hamiltonian are mathematically tractable, so we can obtain compact expressions that are amenable to (possibly computer aided) analytical techniques. To this end, we reclassify the operators of the conformal basis by organizing them in terms of a new quantum number defined by

$$J = \Delta - n \quad (2.4)$$

This number expresses the total number of excess chiral derivatives have been applied on any given operator. We remind the reader that the lowest primary in any particle sector n , must have conformal dimension great or equal to n . For a free boson, there is only one such operator at each particle sector, namely $(\partial\phi)^n$, and since $\partial\phi$ are our basic building blocks, this operator obviously has $J = 0$, since it is only composed out of those.

Every other operator in that sector needs to be built by putting more derivatives on each fundamental field. In every particle sector, there is only a finite number of operators of a given J . Interestingly, for a given J and as one increases the particle number, the number of operators $N(J, n)$ eventually stops growing. In other words,

$$N(J, n) = C(J) \quad , \quad n \geq n_0(J) \quad (2.5)$$

where $n_0(J)$ is a simple function. This means that only a few infinite families of operators can be constructed for each value of J , and that depends on their position on the recursive tree, generated by the double trace algorithm used in [4]. Somewhat surprisingly, for $J = 0, 2, 3$, there is only one operator per particle sector, so their infinite families can be built with no extra effort, and are simply labeled by their particle number. There are no $J = 1$ operators, since any monomial of the form $(\partial\phi)^{n-1}\partial^2\phi$ is a descendant of $(\partial\phi)^n$ and is, therefore, redundant.

A good choice of the A_n for our purposes is the classic harmonic oscillator coherent state choice

$$A_n = \frac{1}{\sqrt{n!}} \quad (2.6)$$

This choice has multiple advantages: firstly, it allows the sum to converge for arbitrary complex argument. Had we chosen $A_n = 1$, for example, the matrix elements of this state would have a finite radius of convergence, giving rise to a divergence at $z = 1$. This doesn't necessarily constitute a problem, since the variational ansatz is still capable of producing an energy minimum, however, such a choice doesn't allow one to have a state that is centered around a particular sector; the probability of such a state to be in a highly excited particle number state is always much lower than the probability of being in lower particle numbers. The classic choice for A_n does not suffer from this problem; the probability distribution defined above presents with a maximum at $\bar{n} \approx |z|^2$ and its full width at half maximum is

$\approx 2\sqrt{n \ln 2}$ as the particle number goes to infinity. Increasing the width further could be beneficial for our purposes, but so far we have not been able to construct such a choice of A_n that is convenient. Finally, this choice allows for simple physical interpretation of the variational ansatz and some simplifications in the calculations, asymptotically, as $|z| \rightarrow \infty$.

We are now ready to construct the $J = 0$ coherent state, using $\mathcal{O}_n = (\partial\phi)^n$:

$$|z; J = 0\rangle = e^{-|z|^2/2} \sum_{n=0}^{\infty} \frac{z^n}{\sqrt{n!}} |(\partial\phi)^{n+1}, p\rangle \quad (2.7)$$

A big advantage to considering states with definite J is that the matrix elements between their constituent states can be computed analytically for any n . Let us start by computing the normalization factor required so that the states obey (2.3):

$$\langle (\partial\phi)^n, p' | (\partial\phi)^n, p \rangle = 2\pi\delta(p - p') \frac{n! p^{2n-1}}{(4\pi)^n N_n^2 \Gamma(2n)} \quad (2.8)$$

from which we infer that

$$N_n^2 = \frac{\pi p^{2n-2} \Gamma(n+1)}{(4\pi)^n \Gamma(2n)} \quad (2.9)$$

A good place to start is to consider the Hamiltonians examined in previous work

$$H_1 = \int dx \left(\frac{m^2}{2!} \phi^2 + \frac{\lambda_3}{3!} \phi^3 + \frac{\lambda_4}{4!} \phi^4 \right) , \quad H_2 = \int dx \left(\frac{m^2}{2!} \phi^2 + \frac{\lambda_4}{4!} \phi^4 + \frac{\lambda_6}{6!} \phi^6 \right) \quad (2.10)$$

and the goal is to compute the variational energy

$$E(z) = \langle z | H | z \rangle \quad (2.11)$$

Since the coherent state (2.7) does not contain the vacuum and vacuum triviality is assumed, we expect that minimizing the variational energy will yield an upper bound on the value of the energy of the gap.

We need to compute the matrix elements $\langle (\partial\phi)^n | V_k | (\partial\phi)^{n+m} \rangle$, where V_k is the interaction term

$$V_k = \int dx \frac{\phi^k}{k!} \quad (2.12)$$

Here are the first few non-zero matrix elements

$$\begin{aligned} \langle (\partial\phi)^n | V_2 | (\partial\phi)^n \rangle &= n(2n-1) \\ \langle (\partial\phi)^n | V_3 | (\partial\phi)^{n+1} \rangle &= (8\pi)^{-1/2} n \sqrt{n(n+1)(2n+1)} \\ \langle (\partial\phi)^n | V_4 | (\partial\phi)^n \rangle &= \frac{n(n-1)(2n-1)}{8\pi} \\ \langle (\partial\phi)^n | V_4 | (\partial\phi)^{n+2} \rangle &= \frac{(n+1)\sqrt{n(n+2)(2n+1)(2n+3)}}{24\pi} \\ \langle (\partial\phi)^n | V_5 | (\partial\phi)^{n+1} \rangle &= \frac{(n-1)n\sqrt{n(n+1)(2n+1)}}{2\sqrt{2}(4\pi)^{3/2}} \\ \langle (\partial\phi)^n | V_5 | (\partial\phi)^{n+3} \rangle &= \frac{(n+1)(n+2)}{12\sqrt{2}(4\pi)^{3/2}} \sqrt{\frac{n(3+n)(3+2n)(5+2n)}{1+2n}} \\ \langle (\partial\phi)^n | V_6 | (\partial\phi)^n \rangle &= \frac{n(n-1)(n-2)(2n-1)}{6(4\pi)^2} \\ \langle (\partial\phi)^n | V_6 | (\partial\phi)^{n+2} \rangle &= \frac{(n^2-1)\sqrt{n(n+2)(2n+1)(2n+3)}}{12(4\pi)^2} \\ \langle (\partial\phi)^n | V_6 | (\partial\phi)^{n+4} \rangle &= \frac{(n+2)(n+3)}{5!(4\pi)^2} \sqrt{\frac{n(4+n)(3+2n)(5+2n)(7+2n)}{1+2n}} \end{aligned} \quad (2.13)$$

A general formula that generates the above results (without the simplifications) is given by

$$\begin{aligned} \langle (\partial\phi)^m | V_n | (\partial\phi)^{m+n-2k} \rangle &= \frac{\Gamma(n-1)\Gamma(m-k+1)\binom{m}{k}\binom{m+n-2k}{n-k}}{(4\pi)^{n/2-1}\Gamma(k)\Gamma(n-k)\Gamma(2m+n-2k-1)} \times \\ &\times \sqrt{\frac{\Gamma(2m)\Gamma(2m+2n-4k)}{\Gamma(m+1)\Gamma(m+n-2k+1)}} \end{aligned} \quad (2.14)$$

Using these matrix elements we can compute the variational energy gain from each term in the Hamiltonian. Generally, for a given power of the field ϕ^n , there are several contributions to the matrix element, coming from matrix elements between operators with different particle numbers:

$$\langle z|V_n|z\rangle = \sum_{k=1}^{\lfloor n/2 \rfloor} (z^{n-2k} + (z^*)^{n-2k}) e^{-|z|^2} \sum_{m=0}^{\infty} \frac{|z|^{2m}}{\sqrt{m!(m+n-2k)!}} \langle (\partial\phi)^{m+1}|V_n|(\partial\phi)^{m+1+n-2k}\rangle \quad (2.15)$$

To organize our exposition optimally, we adopt the following rewriting of the above equation using new notation and setting $z = |z|e^{i\theta}$:

$$\langle z|V_n|z\rangle = \sum_{k=1}^{\lfloor n/2 \rfloor} \cos(n-2k)\theta \mathcal{F}_{nk}(|z|) \quad (2.16)$$

with

$$\mathcal{F}_{nk}(|z|) = |z|^{n-2k} e^{-|z|^2} \sum_{m=0}^{\infty} \frac{|z|^{2m}}{m!} R_m^{nk} \quad (2.17)$$

$$R_m^{nk} = \sqrt{\frac{m!}{(m+n-2k)!}} \langle (\partial\phi)^{m+1}|V_n|(\partial\phi)^{m+1+n-2k}\rangle \quad (2.18)$$

The coefficients in the summation can always be written as the square root of a rational function such that

$$(R_m^{nk})^2 = \frac{P(n)}{Q(n)} \quad \deg P - \deg Q = 2k + 2 \quad (2.19)$$

The variational energy contributions to H_1, H_2 can be computed from the expressions for the matrix elements provided above. In fact, the diagonal particle number contributions of each power of ϕ can be computed exactly, and they are polynomials in $|z|$:

$$\langle z|m^2 V_2|z\rangle = m^2(1 + 5|z|^2 + 2|z|^4) \quad (2.20)$$

$$\langle z|\lambda_3 V_3|z\rangle = \frac{\lambda_3}{\sqrt{8\pi}} (z + z^*) e^{-|z|^2} \sum_{n=0}^{\infty} \frac{|z|^{2n}}{n!} (n+1) \sqrt{(n+2)(2n+3)} \quad (2.21)$$

$$\begin{aligned}
\langle z|\lambda_4 V_4|z\rangle &= \frac{\lambda_4}{8\pi}(9|z|^2 + 6|z|^4 + 2|z|^6) + \\
&\frac{\lambda_4}{24\pi}(z^2 + (z^*)^2)e^{-|z|^2} \sum_{n=0}^{\infty} \frac{|z|^{2n}}{n!} \sqrt{(n+2)(n+3)(2n+3)(2n+5)}
\end{aligned} \tag{2.22}$$

$$\begin{aligned}
\langle z|\lambda_6 V_6|z\rangle &= \frac{\lambda_6}{6(4\pi)^2}(15|z|^4 + 13|z|^6 + 2|z|^8) + \\
&\frac{\lambda_6}{12(4\pi)^2}(z^2 + (z^*)^2)e^{-|z|^2} \sum_{n=0}^{\infty} \frac{|z|^{2n}}{n!} n \sqrt{(n+2)(n+3)(2n+3)(2n+5)} + \\
&\frac{\lambda_6}{5!(4\pi)^2}e^{-|z|^2}(z^4 + (z^*)^4) \sum_{n=0}^{\infty} \frac{|z|^{2n}}{n!} \sqrt{\frac{(n+3)(n+4)(n+5)(2n+5)(2n+7)(2n+9)}{(n+2)(2n+3)}}
\end{aligned} \tag{2.23}$$

3 Asymptotics of expectation values

The contributions of the off-diagonal elements contain square roots of polynomials and that makes their evaluation in closed form quite difficult; however, it is possible to find a large $|z|$ asymptotic expansion by expanding the polynomial under the square root for large n . Generally, the coefficients (2.19) can be obtained by expanding the quantity under the square root at large n :

$$R_m^{nk} = \sum_{M=-k-1}^{\infty} \frac{B_M^R}{n^M} \tag{3.1}$$

We seek to substitute the series into the summation and resum, but we notice that in its current form the series doesn't have a simple analytic solution, especially when it comes to terms with negative powers. Therefore, it is sensible to expand the series in terms of the basis functions

$$R_m^{nk} = \sum_{\ell=-k-1}^{\infty} C_{\ell}^R \frac{n!}{(n+\ell)!} \tag{3.2}$$

If the coefficients C_ℓ^R of this rather unusual expansion are known, then the series can be easily summed term by term, since the following relation

$$\sum_{n=0}^{\infty} \frac{z^{2n}}{(n+\ell)!} = \frac{e^{z^2} - \sum_{n=0}^{\ell-1} \frac{z^{2n}}{n!}}{z^\ell} \quad (3.3)$$

holds for all ℓ , with the usual convention that the sum in the numerator is zero if $\ell \leq 0$. It is not very difficult to obtain (at least numerically) an expression for C^R if the Laurent series coefficients B^R are known; all one has to do is express the basis functions (3.2) in terms of powers of n . The mapping of the finite number of divergent terms of the series is trivialized by noting that one can express powers in terms of falling factorials by using Stirling numbers of the second kind:

$$n^r = \sum_{\ell=0}^r S(r, \ell) \frac{n!}{(n-\ell)!} \quad (3.4)$$

Accordingly, for negative values it can be shown by direct computation using partial fractions that

$$\frac{n!}{(n+k)!} = \sum_{\ell=k}^{\infty} \frac{(-1)^{k+\ell} S(\ell, k)}{n^\ell} \quad (3.5)$$

and the inverse of this relationship can be shown to be given by a similar sum involving the Stirling numbers of the first kind:

$$\frac{1}{n^k} = \sum_{q=k}^{\infty} (-1)^{k+q} s(q, k) \frac{n!}{(n+q)!} \quad (3.6)$$

This in turn gives us a relation between the coefficients of (3.1) and (3.2):

$$C_\ell^R = \begin{cases} \sum_{M=1}^{\ell} (-1)^{\ell+M} s(\ell, M) B_M^R & \ell > 0 \\ \sum_{M=-k-1}^{-\ell} S(-M, -\ell) B_M^R & \ell \leq 0 \end{cases} \quad (3.7)$$

As an example, we show the calculation for (2.21):

$$(n+1)\sqrt{(n+2)(2n+3)} = \sqrt{2} \left(n^2 + \frac{11}{4}n + \frac{55}{32} + \frac{3}{2^7 n} - \frac{85}{2^{11} n^2} \right) + \mathcal{O}(n^{-3}) \quad (3.8)$$

Applying the procedure outlined above, we can generate an arbitrary number of terms in the expansion and resum term by term for the result:

$$\langle z|V_3|z\rangle = \frac{\lambda_3}{\sqrt{4\pi}} 2 \cos \theta \left(|z|^5 + \frac{15}{4}|z|^3 + \frac{55}{32}|z| + \frac{3}{128} \frac{1 - e^{-|z|^2}}{|z|} - \frac{37}{2048} \frac{1 - (1 + |z|^2)e^{-|z|^2}}{|z|^3} + \mathcal{O}(|z|^{-5}) \right) \quad (3.9)$$

The magic about this kind of expansion is that one can get a very good approximation of the value of the full series by just using a few terms; surprisingly, it turns out that the limit $\mathcal{F}_{31}(0) = \sqrt{6}$ is reproduced to good accuracy by just using the asymptotic expansion provided above. It is nevertheless prudent to use the series evaluated to a few hundred terms near the origin to maximize the accuracy to which the series is represented. To wit, it can be shown that the error we commit by truncating the series to the first N terms is bounded above by

$$e_N(z) := \left| z e^{-|z|^2} \sum_{n=N}^{\infty} \frac{|z|^{2n}}{n!} (n+1) \sqrt{(n+2)(2n+3)} \right| < \sqrt{2} \frac{|z|^{2N+1}}{(N-2)!} \left(1 + \frac{4}{N-1} + \frac{2}{N(N-1)} \right) \quad (3.10)$$

For a given choice of the coherent state parameter z that is sufficiently large, we see that the bound becomes maximally loose for $N \approx |z|^2$. This is a hint that to replicate the function well at the given position we need to include at least that many terms in the sum. Using the truncated series to reproduce the function at large $|z|$ thus quickly becomes impractical, and the asymptotic series is required past a certain point to obtain a good approximation of the true value.

Thanks to the results above, we can now approximate the functions \mathcal{F}_{nk} with excellent accuracy throughout their range. Importantly, due to the nature of the asymptotic series,

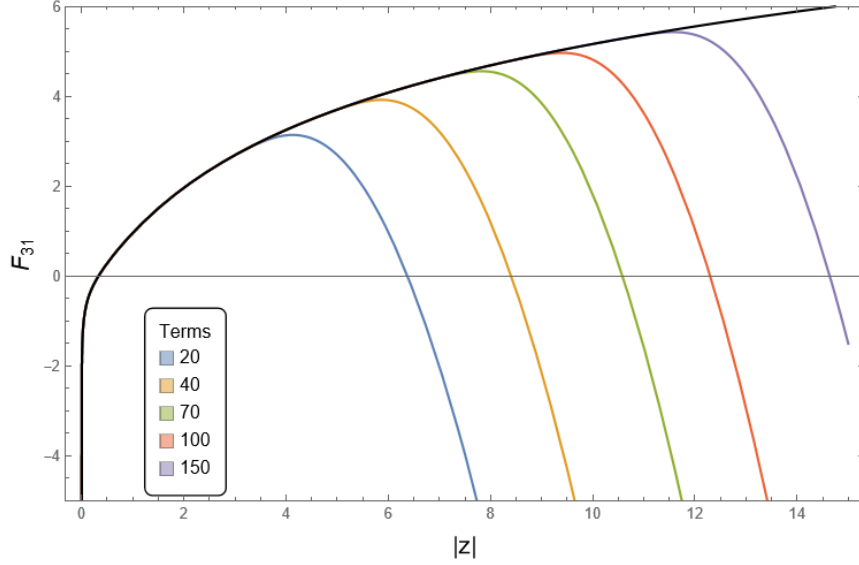


Figure 1: Plot of various approximations to the function F_{31} . Colored curves represent the values provided by truncations of the infinite series for F_{31} , while the black curve represents our best estimate for the function, which involves both a high-order truncation of the series and a high-order truncation of its asymptotic series at infinity.

the error is well controlled at infinity as well, so this means that the relative error to which we are approximating the function vanishes at infinity as well. The most difficult range to achieve reasonable accuracy is the intermediate regime, where the Taylor series breaks down and the error of the asymptotic series is still relatively large. To mitigate the errors in the evaluations of the functions, we have used truncated Taylor series with a large number of terms kept, N . These series are good representations for $|z| \lesssim \sqrt{N}$, past which point they diverge from the true values. Past that point, the asymptotic series needs to be used. To generate values for our function, we use a combination of a modest truncation of F_{nk} along with the asymptotic approximation, for a minimum of 15 digits of accuracy. More specifically, the Taylor series is used for values less than $|z| \sim 7 - 8$, and the asymptotic series for any other value. The error of the asymptotic series can be seen in Fig. 2, which shows that our choice for the cutoff is rather conservative- however, evaluating large sums that converge to within $|z| < 10$ requires a minimum of $N = 200$ terms in the series, which requires a lot of computational resources to evaluate.

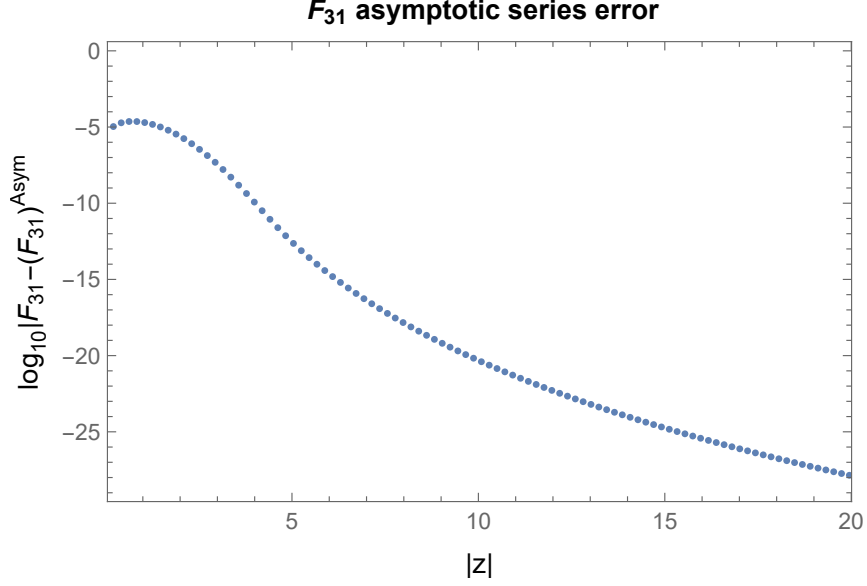


Figure 2: Plot of the error of the asymptotic approximation to F_{31} for various values of the variational parameter. Here the asymptotic value of the function is compared to a Taylor series that has converged to the true value > 30 digits in the range of interest (the evaluations have been done with increased precision). Even for small $|z|$, the asymptotic approximation is excellent, and the error becomes smaller as $|z|$ increases, due to the fact that we have included all divergent terms in the asymptotic series in our approximation. To generate values for our function, we use a combination of a modest truncation of F_{nk} along with the asymptotic approximation, for a minimum of 15 digits of accuracy.

As shown in the figure , the function can be easily represented to a minimum of 8 digits accuracy, by using the explicit series for some $|z| < z_0$ and the asymptotic approximation for $|z| > z_0$.

The asymptotic expansion for the contributions of ϕ^4, ϕ^6 are given by

$$\begin{aligned} \langle z | \lambda_4 V_4 | z \rangle &= \frac{\lambda_4}{8\pi} (9|z|^2 + 6|z|^4 + 2|z|^6) + \\ &\quad \frac{\lambda_4}{12\pi} \cos 2\theta \left(2|z|^6 + 11|z|^4 + \frac{19}{2}|z|^2 - \frac{1}{16|z|^2} + \dots \right) \end{aligned} \quad (3.11)$$

$$\begin{aligned} \langle z | \lambda_6 V_6 | z \rangle &= \frac{\lambda_6}{6(4\pi)^2} (2|z|^8 + 13|z|^6 + 15|z|^4) + \\ &\quad \frac{\lambda_6}{6(4\pi)^2} \cos 2\theta \left(2|z|^8 + 15|z|^6 + \frac{41}{2}|z|^4 - \frac{1}{16} + \dots \right) + \\ &\quad \frac{\lambda_6}{60(4\pi)^2} \cos 4\theta \left(2|z|^8 + 21|z|^6 + 49|z|^4 + 12|z|^2 - \frac{17}{2} + \dots \right) \end{aligned} \quad (3.12)$$

4 $J = 0$ coherent state: Results

Asymptotically, the contribution for the interaction ϕ^n is a polynomial of degree $n + 2$ in $|z|$, and morally speaking, its structure is rather simple. This is further corroborated by the fact that the asymptotic expansion is valid to within 5 digits throughout the entire range of the variational parameter, giving rise to a somewhat predictable pattern in the variational energy. Furthermore, we note that any *negative* contribution to the Hamiltonian H_1 must come from the minimization procedure. The sourcing terms are of course the quantities $z^k + (z^*)^k = 2|z| \cos k\theta$. These quantities have the potential to give a large negative contribution to the potential $E(z)$ after minimization, causing the symmetry to break at large enough values of the odd couplings. One might have hoped that the above variational approximation would give rise to a zero mass gap in the case of zero cubic coupling. However, as we will see below, this variational ansatz is not enough to reproduce the physics at strong coupling.

The total variational energy for the ϕ^4 theory is given by summing together (2.20), (2.21), (2.22) and when written in terms of $|z|, \theta$, it reads

$$E(|z|, \theta) = m^2 \mathcal{F}_{21}(|z|) + \lambda_4 \mathcal{F}_{42}(|z|) + \lambda_3 \cos \theta \mathcal{F}_{31}(|z|) + \lambda_4 \cos 2\theta \mathcal{F}_{41}(|z|) \quad (4.1)$$

We can maximize this quantity in terms of θ explicitly, since we can easily show that the minimizer θ^* of the function $f(\theta) = a \cos^2 \theta + b \cos \theta$ satisfies

$$\cos \theta^* = -u(b - 2a) - \frac{b}{2a}u(2a - b) \quad (4.2)$$

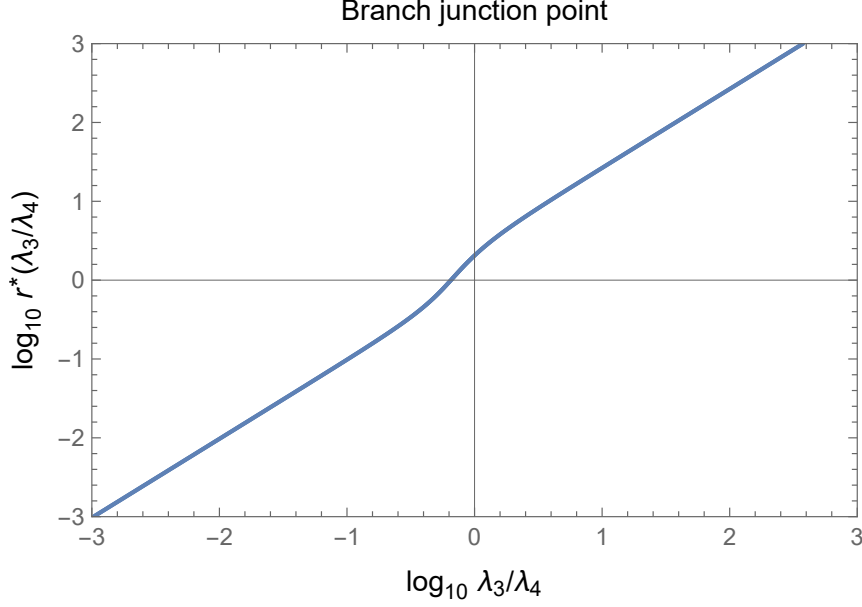


Figure 3: Plot of the branch switching curve in terms of the slope λ_3/λ_4 . For values of $r > r^*$ (above the curve), evaluations of (4.4) require evaluation of the upper branch, while all values below the curve shown use the lower branch.

Applied in our case, we find that we must set

$$\cos \theta = \begin{cases} -1 & , \quad \frac{\lambda_3 \mathcal{F}_{31}}{4\lambda_4 \mathcal{F}_{41}} > 1 \\ -\frac{\lambda_3 \mathcal{F}_{31}}{4\lambda_4 \mathcal{F}_{41}} & \text{else} \end{cases} \quad (4.3)$$

And hence finding the variational energy is reduced to the one variable optimization problem of the function

$$V(r) = \begin{cases} m^2 \mathcal{F}_{21}(r) + \lambda_4 (\mathcal{F}_{42}(r) - \mathcal{F}_{41}(r)) - \frac{\lambda_3^2}{8\lambda_4} \frac{(\mathcal{F}_{31}(r))^2}{\mathcal{F}_{41}(r)} & , \quad \frac{\lambda_3 \mathcal{F}_{31}}{4\lambda_4 \mathcal{F}_{41}} < 1 \\ m^2 \mathcal{F}_{21}(r) + \lambda_4 (\mathcal{F}_{42}(r) + \mathcal{F}_{41}(r)) - \lambda_3 \mathcal{F}_{31}(r) & , \quad \text{else} \end{cases} \quad (4.4)$$

Which branch will be used for the evaluation of the variational energy at a given value of the variational parameter depends on the ratio λ_3/λ_4 . In Fig. 3 shows the junction point,

defined to be the solution of the equation

$$r^* : \frac{\mathcal{F}_{41}(r^*)}{\mathcal{F}_{31}(r^*)} = \frac{\lambda_3}{4\lambda_4} \quad (4.5)$$

For values of the parameter higher than the branching curve, the upper branch is used, while values lower than the branching curve require the lower branch.

Also, this reveals the somewhat simple semiclassical structure of the ansatz: all interesting physics is controlled by the combination λ_3^2/λ_4 , which has ubiquitously shown up in previous work in the weakly coupled symmetry broken regime of the theory. The lower branch of $V(r)$ is trivial, in the sense that asymptotically it has the structure of a symmetry broken ϕ^6 potential with fixed ratio of cubic and quintic terms. Eventually, at large enough λ_3 , a new minimum must descend and drive the system to vacuum breakdown. The upper branch is a somewhat more non-trivial looking sextic potential, in the sense that, asymptotically, not only is the sextic term weaker, but the transition is driven by a negative quartic term proportional to the aforementioned combination of couplings. The upper branch is selected whenever $r \gtrsim \mathcal{O}(\lambda_3/\lambda_4)$, so we expect that it dominates completely for small cubic couplings.

Conveniently, we only need to explore the above minimization problem numerically in the projective \mathbb{RP}^2 coupling space $(m^2; \lambda_3; \lambda_4) = (1; \lambda_3/m^2; \lambda_4/m^2)$, since when the couplings are simultaneously scaled the mass matrix scales proportionally. Furthermore, examining the points outside of the projective plane $(0; 1; \lambda), (0; 0; 1)$ is tricky, since these theories are strongly coupled and require special treatment.

The first result of our computational exploration of the minima in the projective coupling space defined above is shown in Fig. 4. One can convince oneself by some manual exploration of the minimizing values of the energy that the variational gap mass will become negative for large enough values of the coupling, and the figure summarizes our simula-

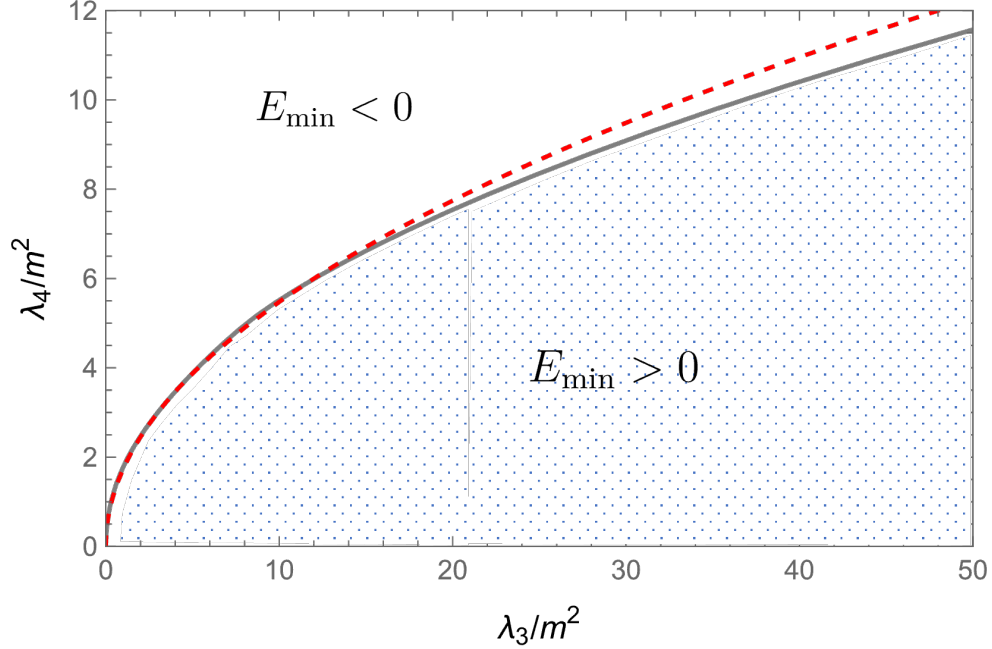


Figure 4: Plot of the curve in projective coupling space where the gap closes. At this line, the LCT trivial vacuum ansatz cannot hold anymore. The transition line follows the expected semiclassical transition $\lambda_3^2 = 3\lambda_4$ closely for smaller couplings, and slightly deviates at higher couplings. However, contrary to expectations from simulations using the truncated LCT Hamiltonian, the gap does not close for $\lambda_3 = 0$, indicating that the variational ansatz needs to be refined.

tions that aimed to find the curve where the gap mass becomes exactly zero. The resulting curve follows the expectations from the semiclassical analysis well, but it fails to reproduce the phenomenology at strong quartic coupling, indicating that the ansatz needs to be refined. It can be shown that a similar result is obtained by a mean field calculation in lightcone quantization, that includes vacuum zero modes in terms of *single particle excited modes only* suggesting that the calculation is morally equivalent to saying that semiclassically, including modes of higher momentum or modes of higher particle number is morally equivalent.

5 Improving the $J = 0$ variational ansatz

From previous work, it is known that the basis $\{(\partial\phi)^n\}$ indicates a breakdown of the lightcone vacuum ansatz at strong coupling, even at finite Δ_{\max} . However, a variational

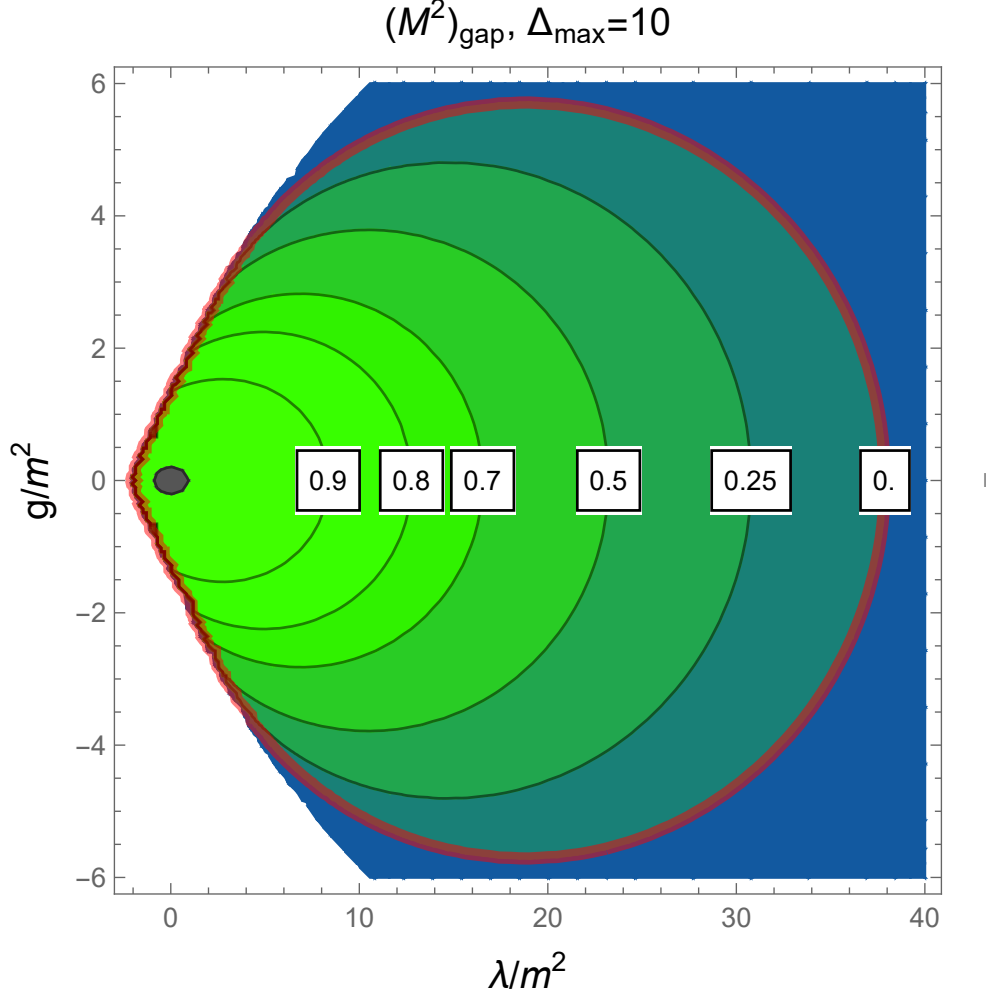


Figure 5: Plot of the gap versus the cubic and quartic coupling ratios. One readily sees the vacuum ansatz breakdown, shown by the red curve, which happens both at large cubic or large quartic coupling. The dark dot marks the free particle, and shows that the perturbative phase transition is not reproduced as precisely as with variational techniques.

ansatz like the one in section 4 does not reproduce the expected closed petal like shape that we have come to expect from large Δ_{\max} simulations with the full bosonic basis. We conclude that the variational ansatz needs further refinement to approximate the ϕ^4 transition. Looking at simulations at high Δ_{\max} using only $J = 0$ operators, we note that this partial basis already sees a phase transition at strong coupling, unlike the ansatz posited. This is already apparent at very small truncations of the $J = 0$ partial basis, as in Fig. 5.

By examining the structure of the eigenvector components of the lowest eigenvalue, we no-

tice, as expected, that there is a clear divide between odd and even operators; in particular when $g \ll \lambda$, the eigenvector is primarily weighted on the odd operators, respecting its (exact when $g = 0$, approximate otherwise) \mathbb{Z}_2 symmetry. The eigenvector is overwhelmingly composed of the single particle state $|\partial\phi, p\rangle$; this makes sense as the single particle state is an exact eigenstate at the origin. As one increases the cubic coupling, the weight placed on even states quickly increases. However, we notice that, as long as we stay within the zero gap closed curve, the lowest mass eigenvectors remain relatively predictable: as a matter of fact we see an alternating sign structure in both odd and even sectors and an exponential decay at large particle numbers. In our ansatz, the asymptotic decay at large particle number is super-exponential instead, as $z^{2n}/n! \sim e^{-n \ln n + (2 \ln |z| + 1)n}$, however, it captures qualitatively the low particle sector dynamics, which are the most important from the LCT perspective. However, it should not be forgotten that asymptotics at large number matter, especially near the phase transitions; this important element manifests itself as a failure of the truncated LCT Hamiltonian to detect the exact semiclassical transition (it assumes all weights beyond Δ_{\max} are zero). On the other hand, our variational ansatz has no issue representing it, due to the fact that the weighting factor we are using can have a nontrivial maximum and can therefore represent well eigenvectors that have the majority of their support around a state different than the first state.

Our primary goal is to write down an ansatz that can exhibit vacuum breakdown at strong coupling in the same way as our basis.

References

- [1] S. S. Chabysheva, Few Body Syst. **55**, 479-484 (2014) doi:10.1007/s00601-014-0884-5 [arXiv:1402.0222 [hep-ph]].
- [2] J. S. Rozowsky and C. B. Thorn, Phys. Rev. Lett. **85**, 1614-1617 (2000) doi:10.1103/PhysRevLett.85.1614 [arXiv:hep-th/0003301 [hep-th]].
- [3] S. S. Chabysheva and J. R. Hiller, Phys. Rev. D **79**, 096012 (2009) doi:10.1103/PhysRevD.79.096012 [arXiv:0903.1239 [hep-ph]].
- [4] N. Anand, A. L. Fitzpatrick, E. Katz, Z. U. Khandker, M. T. Walters and Y. Xin, [arXiv:2005.13544 [hep-th]].